Advanced multichannel submersible probe for autonomous high-resolution *in situ* monitoring of the cycling of the potentially bioavailable fraction of a range of trace metals

Mary-Lou Tercier-Waeber [a,*], Fabio Confalonieri [b], Melina Abdou [a,c], Lionel Dutruch [c], Cécile Bossy [c], Marianna Fighera [d], Eric Bakker [a], Flavio Graziottin [b], Peter van der Wal [d], Jörg Schäfer [c]

[a] *University of Geneva, Dept. of Inorganic and Analytical Chemistry, 1211 Geneva 4, Switzerland*
[b] *Idronaut Srl, Via Monte Amiata 10, 20047 Brugherio (MB), Italy*
[c] *University of Bordeaux, UMR CNRS 5805 EPOC, 33615 Pessac, France*
[d] *Ecole Polytechnique Fédérale de Lausanne (EPFL), Neuchâtel, Switzerland*

ARTICLE INFO

ABSTRACT

We report here on the development and application of a submersible, compact, low power consumption, integrated multichannel trace metal sensing probe (TracMetal). This probe is unique in that it allows high-resolution, simultaneous *in-situ* measurements of the potentially bioavailable (so-called dynamic) fraction of Hg(II), As(III), Cd(II), Pb(II), Cu(II), Zn(II). The TracMetal incorporates nanostructured Au-plated and Hg-plated gel-integrated microelectrode arrays. In addition to be selective to the fraction of metal potentially bioavailable, they offer protection against fouling and ill-controlled convective interferences. Sensitivities in the low pM for Hg(II) and sub-nM for the other target trace metals is achieved with precision $\leq$ 12%. The TracMetal is capable of autonomous operation during deployment, with routines for repetitive measurements (1-2 h^{-1}), data storage and management, data computer visualization, and wireless data transfer. The system was successfully applied in the Arcachon Bay, to study the temporal variation of the dynamic fraction of the trace metals targeted. The *in situ* autonomous TracMetal measurements were combined with *in situ* measurements of the master bio-physicochemical parameters and sample collection for complementary measurements of the dissolved metal concentrations, organic matter concentrations and proxy for biological activities. The integration of all data revealed that various biotic and abiotic processes control the temporal variation of the dynamic fractions of the target metals (Me$_{dyn}$). The difference in the percentage of the dynamic forms of the metals studied and the short-term processes influencing their variation highlight the TracMetal potentiality as metal bioavailability-assessment sentinel to achieve comprehensive environmental monitoring of dynamic aquatic systems.

1. Introduction

Trace metals in aquatic ecosystems are highly reactive and their dynamics play critical roles in the functioning of ecosystems. Metal and metalloids such as mercury, lead and arsenic may be highly toxic even at low concentrations, whereas other trace metals such as iron, copper, zinc, cadmium, manganese, cobalt, molybdenum are essential micro-nutrients, especially for algal communities. Within an optimal concentration range, they mediate vital biochemical reactions including carbon fixation, nitrification/denitrification, remineralization of organic matter (Anderson et al., 2014; Morel et al., 2003; Sunda, 2012). Below or above this optimal range, detrimental effects occur owing to deficiency or excess. Each algal species shows an optimal development at a specific trace metal concentration (Ho et al., 2003; Twining and Baines, 2013). The concentration and speciation of metals in aquatic ecosystems affects the growth and turnover rate of phytoplankton and modulates phytoplankton species composition (Anderson et al., 2014; Baeyens et al., 2018; Morel et al., 2003; Sunda, 2012), therefore affecting the productivity of entire food webs and the rate of particulate carbon export to the deep ocean. Bioaccumulation of trace metal species contributes to

harmful algal blooms and the production of powerful toxins that those induce (Maldonato et al., 2002).

Assessing the impact of metals on aquatic ecosystems and ultimately human health is challenging for several reasons. Most dissolved metals are present at sub-nanomolar concentrations in surface freshwater, coastal areas and open ocean (Bruland et al., 2013; Gaillardet et al., 2003). Monitoring subtle variations of bioactive metals therefore requires highly sensitive analyzers. Trace metals are distributed in a variety of redox states and chemical species (speciation) which proportion depend on the physical, chemical and biological conditions of the medium (Baeyens et al., 2011; Tercier-Waeber et al., 2012). Only some metal species are bioavailable (Tercier-Waeber et al., 2012; Zhao et al., 2016). Because geochemical processes in aquatic systems are highly dynamic, the metal fraction available for bio-uptake may vary at hourly time scales (Grand et al., 2019; Luoma and Rainbow, 2011; Tercier-Waeber et al, 2009, 2012). Experimental evidence also suggests that enhanced inputs of metals may influence phytoplankton diversity and growth on an hourly to weekly time scale (e.g. Grand et al., 2019; Twining and Baines, 2013; and references therein). Monitoring dynamic metal cycling at such short time scales is incompatible with discrete sampling approaches. It requires rapid and adaptive *in situ* observations to characterize episodic events and assess their impact (Anderson et al., 2014; Grand et al., 2019; Tercier-Waeber et al., 2012). Furthermore, measurements of potentially bioavailable metal species is of primary concern to conduct realistic risk assessments (Durán and Beiras, 2013; Illuminati et al., 2019; Väänänen et al., 2018). This has been recognized by international environmental administration bodies (EU, US-EPA, Canada, China), stating the need to incorporate metal bioavailability-assessment tools into environmental regulation for ecotoxicology-related environmental quality standards (EQS) and guidelines (EQG) to protect aquatic life and human health (ANZECC, 2000; Merrington et al., 2016; Väänänen et al., 2018).

On-chip Gel Integrated Microelectrodes (GIME) incorporated in a submersible device are, among a few other analytical techniques recently reviewed (Grand et al., 2019), promising trace metal bioavailability-based sensing tools for *in situ* applications. The on-chip GIME consists of an array of microdisk electrodes with radii <10 μm (so-called ultra-microelectrodes) that are electrochemically plated with an appropriate sensing element and covered by a hydrogel membrane (Belmont-Hébert et al., 1998; Buffle and Tercier-Waeber, 2005). When a GIME is interrogated by square wave anodic stripping voltammetry (SWASV), the signal recorded at natural pH is selectively due to the so-called dynamic metal species (Buffle and Tercier-Waeber, 2005; Sigg et al., 2006). This metal fraction includes the free metal ions and the sufficiently labile (complexes of high dissociation rate) and mobile (high diffusion rate) inorganic and organic complexes/species of a few nanometers in size (Buffle and Tercier-Waeber, 2005; van Leeuwen et al., 2005). This fraction is of great importance, as it represents the maximum concentration of dissolved metals that are bioaccessible from solution. Indeed, if diffusional mass transport of the metal in the external medium is the rate limiting step, rather than the uptake through the biological membrane, the labile and mobile metal complexes are expected to contribute to the metal bioavailability (Buffle et al., 2009; Tercier-Waeber et al., 2012; Zhao et al., 2016). The other key features of the GIME are related to the characteristics of the hydrogel membrane (high purity LGL agarose gel) (Belmont-Hébert et al., 1998; Tercier and Buffle, 1996; Tercier-Waeber et al., 2021; Touilloux et al., 2015). Namely, it is inert toward metal cations, neutral oxyanions, negatively charged inorganic metal complexes and oxyanions. It acts as a dialysis membrane excluding the diffusion of inorganic, organic and biological fouling materials toward the sensor surface. It displays anti-convective properties ensuring that mass transport toward the sensor surface is controlled by pure diffusion. These characteristics are essential to obtain a sensor that is reliable and robust enough to be integrated in a submersible probe and applied for *in situ* long-term monitoring.

The first on-chip GIME were developed in the nineties and consisted

of single or 100 interconnected Iridium (Ir)-based microdisk arrays that were plated with mercury (Hg) and integrated in a gel (Belmont-Hébert et al., 1998). Excellent functionality of these Hg-GIME for *in situ* environmental analysis of the dynamic fraction of Cu(II), Pb(II), Cd(II), Zn (II) at sub-nanomolar concentrations has been demonstrated later on by their incorporation in a submersible device, the Voltammetric In situ Profiling system (VIP) developed by Tercier-Waeber et al. (2002) and marketed by Idronaut® (Milan, Italy). This VIP was successfully applied in various terrestrial and marine aquatic systems (e.g. Illuminati et al., 2019; Tercier-Waeber et al., 2002, 2008, 2009; and references therein) and its accuracy for high resolution *in situ* monitoring was demonstrated in a European laboratory inter-comparison exercise (Braungardt et al., 2009). So far, solid-state Hg–Au sensors incorporated in various deployable platforms for *in situ* measurements of Mn(II), Fe(II) are the only other autonomous submersible systems that have been systematically characterized, optimized, validate and applied for trace metal analysis in various environmental studies, (e.g. Tercier-Waeber and Taillefert, 2008; and references therein). Few other systems were reported, however these probes were not sensitive enough for the determination of trace metals in non-polluted waters, and none of them can be used for continuous measurements over a period of time superior to one day (e.g. Buffle and Tercier-Waeber, 2000; and references therein). More recently, newly designed GIME based on 190 to 500 interconnected Ir-based microdisk arrays that were either electrochemically plated with Hg (Hg-GIME) or with gold nanoparticles or filaments (AuNP-GIME, AuNF-GIME) have been developed. The objectives were to improve the Hg-GIME sensitivity (Fighera et al., 2016) and provide GIME sensors for the detection of other hazardous metals. Very recent work has shown that the AuNP-GIME and AuNF-GIME allow quantifying inorganic As(III) and Hg(II) at environmental levels with no or minimal sample pre-treatment (Tercier-Waeber et al., 2020, 2021).

We present here the development and the application of an advanced autonomous electrochemical sensing probe, the TracMetal. The TracMetal is a compact, low power consumption, submersible integrated multichannel trace metal sensing probe. The TracMetal allows for the autonomous, real-time, *in situ* and simultaneous measurements of the dynamic (potentially bioavailable) fraction of Hg(II), As(III), Cd(II), Pb (II), Cu(II), Zn(II). It is based on the newly designed 190-interconnected Hg-GIME and AuNF-GIME (Fighera et al., 2016; Tercier-Waeber et al., 2020, 2021). The GIMEs are incorporated in a three-channel flow-through cell, which is integrated into the TracMetal electronic housing and connected to a multi-channel peristaltic pump. The TracMetal was applied to high-resolution monitoring of the temporal variability of the bioavailable fractions of the six target hazardous metals in the Arcachon Bay, representative of the southwest European Atlantic Coast hosting major coastal protected areas and economic activities (seafood production areas). In parallel, master variables were monitored *in situ*, and water samples were collected for complementary analyses of total dissolved metal concentrations, water composition and proxies for primary production. The integrated data were used to identify and assess the main abiotic and biotic processes that control the temporal concentrations and cycling of the potentially bioavailable (dynamic) fractions of the targeted metals, and to assess their sources in the Arcachon Bay.

This works marks the first time ever that an autonomous electrochemical sensing probe enables to make high accuracy measurements of the dynamic fraction of inorganic As(III) and Hg(II) *in situ* with no or minimum perturbation of the media. It also provides the first data on the concentrations of the dynamic fraction of a range of hazardous trace metals in the Arcachon Bay and their hourly temporal variations reflecting realistic exposure of aquatic organisms.

2. Experimental section

2.1. GIME sensor description and preparation

The chips containing an array of 10x19 interconnected Ir-based

microdisks of 2.5 μm radius were fabricated on silicon wafer by photolithography as reported previously (Fighera et al., 2016; Tercier-Waeber et al., 2020, 2021) and shown in Supporting Information (Fig. S1). The devices were electrochemically plated with appropriate renewable sensing layers and covered with a 150 μm thick agarose gel layer (high purity LGL agarose, Biofinex®-Switzerland). The sensing element for direct detection of the dynamic fraction of inorganic As(III) and Hg(II) (respectively denominated As(III)$_{dyn}$, Hg(II)$_{dyn}$) consisted of gold nanofilaments (AuNF-GIME), while Hg hemispheres (Hg-GIME) were used for direct and simultaneous detection of Cu(II)$_{dyn}$, Cd(II)$_{dyn}$, Pb(II)$_{dyn}$, Zn(II)$_{dyn}$ (Fig. S1). A micro counter-electrode (μCE), of 0.85 mm × 0.55 mm in size, was added to each chip (Fig. S1; Fighera et al., 2016; Tercier-Waeber et al., 2020, 2021). The analytical protocols and conditions used for the preparation of the 190-Hg-GIME and 190-AuNF-GIME and, if required, the renewal of their sensing layers were as previously reported by Belmont-Hébert et al. (1998) and Tercier-Waeber et al. (2020), respectively. They are summarized in Supporting information (SI).

2.2. TracMetal probe description

The TracMetal is comprised of a three integrated-channel flow-through voltammetric cell, an electronic housing and an external peristaltic pump (Fig. 1). Each channel of the flow-through cell incorporates a GIME and a micro-counter electrode on a single chip as well as a mini in-house reference electrode (Fig. 1A). This cell is coupled to the TracMetal electronic housing using dedicated electrical connectors and mechanical devices. The external double-head peristaltic pump, with up to three channels on each head, serves to collect and renew the samples in the individual channels of the flow-through cell prior to the start of a new measurement at the programmed time. This is achieved by running the pump for 2 min (Table S3) at a flow-rate of 4 mL/s that enables to renew 10 times the 0.8 mL volume of the individual channels. It also

enables in-line sample dilution by 20% with 0.1 M NaCl, 0.2 M borate buffer, setting the final concentration of borate buffer at 0.02 M and the sample pH at 7.6, for As(III)$_{dyn}$ detection (Penezić et al., 2020).

The electronic housing incorporates three potentiostats and preamplifiers for simultaneous measurements with the three GIME-TracMetal channels. It also hosts dedicated hardware/software modules as well as communication interfaces for automatic data storage, pressure and temperature sensor connections and measurements; wired and wireless bi-directional control of the TracMetal and data transfer, including diagnose and failure reports (see SI). The borate buffer solution for As(III)$_{dyn}$ measurements was stored in a chirurgical bag. Two in-line oxygen removal systems (Tercier-Waeber and Buffle, 2000) were connected to the inlet of the AuNF-GIMEs cell channels for oxygen removal prior to As(III)$_{dyn}$ and Hg(II)$_{dyn}$ detection. *In situ* detection of Cu(II)$_{dyn}$, Cd(II)$_{dyn}$, Pb(II)$_{dyn}$, Zn(II)$_{dyn}$ in marine waters was performed in the presence of oxygen (Tercier et al., 1998). The power supply of the TracMetal and communication between the system and a laptop computer is via a single armored coaxial cable. The external power required is 12 VDC (9–15 V) and the power consumption is 1.2 W during sampling and measuring step and 0.012 W in sleeping mode between measurements, i.e. much lower compared to the typically 300 W of the commercial benchtop potentiostats (e.g. Ainla et al., 2018). During field trials, the system can be powered with an external widely available 12 VDC - 40 to 50 Ah battery, in addition to an internal rechargeable NiMH 12 VDC-8 Ah battery pack. Each measurement typically consumes 1.5 kJ and 3 kJ when using an electrochemical preconcentration time of respectively 10 and 30 min. Considering one measurement per hour, the external battery provides autonomy of respectively 50 and 25 days, while the internal rechargeable battery pack enables autonomous, continuous field deployment for respectively 8 and 4 days.

The developed firmware and Windows user-friendly management software enables, through menus and mnemonic commands, to set up the TracMetal operating parameters and functions such as fluidic and
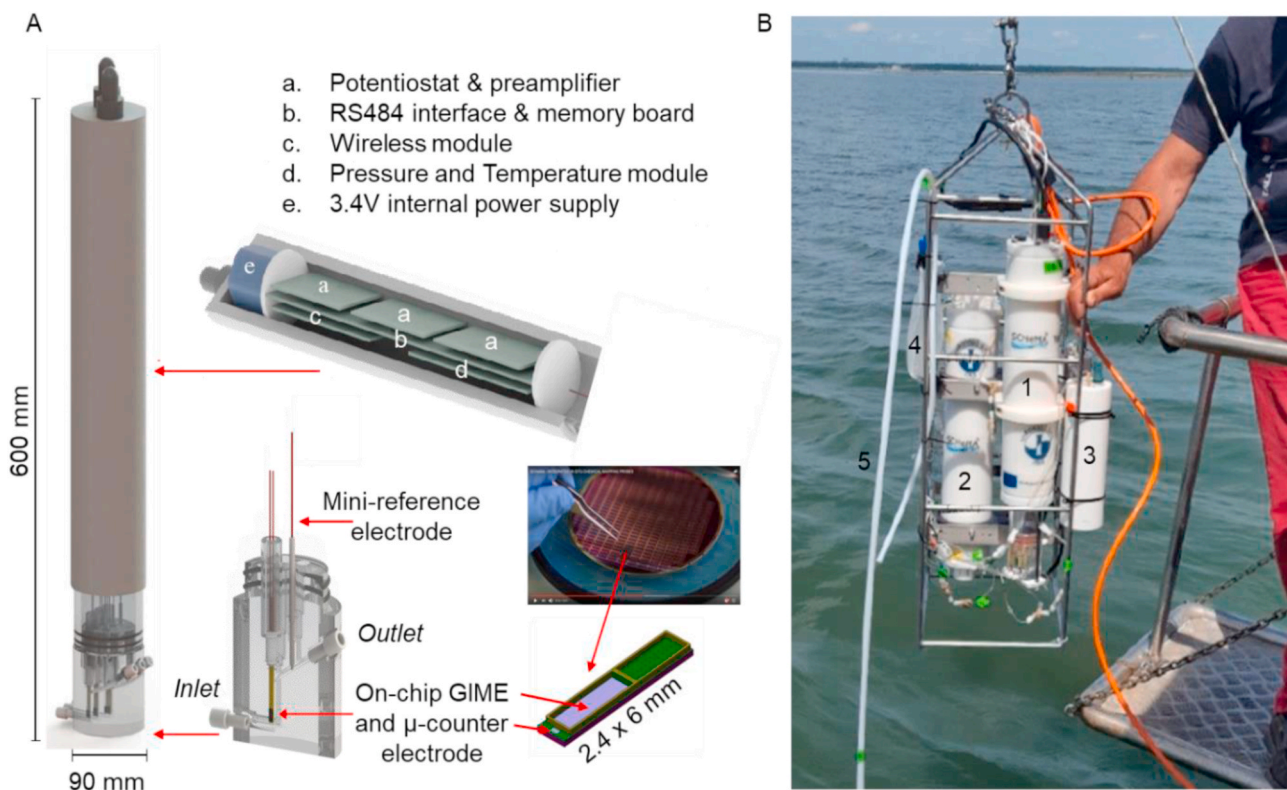

Fig. 1. (A) Scheme of the main components of the TracMetal voltammetric probe. (B) 1, the TracMetal voltammetric probe incorporated into a protective titanium cage together with: 2, the multi-channel double-head submersible pump; 3, submersible on-line oxygen removal system (Tercier-Waeber and Buffle, 2000); 4, chirurgical bag containing the buffer solution for As(III)$_{dyn}$ detection; 5, acid-cleaned Teflon sampling tube used to collect water samples for ancillary measurements.

electrochemical parameters, three-channel independent or simultaneous measurements, smart data processing, and diagnostic and maintenance operations of the probe components (for detail see SI, section S1.3).

2.3. Study area and in situ monitoring site

The Arcachon Bay is a meso-tidal lagoon in southwest France, ~100 km to the south of the Gironde Estuary mouth. It represents an important breeding ecosystem for regional seafood production, especially oysters. On 15–16 May 2017, the TracMetal, coupled to a Idronaut® OS316 multiparameter probe, was deployed at 2.5 m depth from the R/V Planula IV (TGIR FOF) at the Comprian site (44°40.823′N, 1°05.902′W; SI, Fig. S2). The Comprian site is located in a main current channel of the bay, receiving inputs from the Leyre River, run-off from urbanized areas surrounding the lagoon (~90,000 inhabitants), and seawater from the Atlantic Ocean.

2.4. In situ measurements of the dynamic metal fractions and master variables

In situ SWASV monitoring of the dynamic (potentially bioavailable) fraction of the six trace metals (Me$_{dyn}$) were performed using one Hg-GIME (TracMetal channel 1) and two AuNF-GIME (TracMetal channels 2 and 3). Hourly autonomous measurements of the Me$_{dyn}$ were performed simultaneously on the three TracMetal individual channels during a 24 h cycle. This was achieved using the optimized measurement protocols and analytical conditions for sample collection and the subtractive SWASV trace metal detection reported in SI (section S1.3 and Table S3). Under these SWASV conditions, Cu(II) and Cl$^-$ interferences are well controlled (Tercier-Waeber et al., 2020, 2021), and the electrochemical Hg(II) preconcentration performed in underpotential deposition (UPD) condition prevents change in the AuNF substrate due to the formation of Hg–Au amalgam (Tercier-Waeber et al., 2021). The detection limits and precision are suitable for *in situ* detection and quantification of all the metals in coastal zones and area influenced by anthropogenic and freshwater inputs (see SI, Table S5). Each measuring channel was calibrated in the field laboratory prior and after the field deployment using synthetic suprapure electrolytes spiked with increasing concentrations of metals as described in SI (section S1.5). Change in sensitivities were <8% for all metals reflecting the reliability of the GIME sensors and the absence of biofouling. Metal concentrations were determined from the SWASV metal peak current intensities corrected for temperature changes (SI, section S1.5) using the average calibration slopes. Vertical error bars in the graphs represent the average %RSD (8% for Cu(II), Cd(II), Pb(II); 11% for As(III); 12% for Hg(II) and Zn(II)) determined from on-board triplicate measurements in a freshly collected sample before (low-tide) and after (high-tide) the 24 h measurement cycle, i.e.: the estimated errors one may expect from the Hg-GIME and AuNF-GIME SWASV measurements.

The master bio-physicochemical variables (temperature, pH, dissolved O$_2$, salinity, turbidity, chlorophyll *a* (chl*a*) were recorded *in situ* at 15 min time intervals with the Idronaut® Ocean Seven 316Plus (OS316) multiparameter probe coupled to the TracMetal.

2.5. Sample collection and laboratory ancillary measurements

Hourly sampling was performed in parallel to the TracMetal *in situ* measurements for complementary measurements of total dissolved metal concentrations (Me$_{diss}$), dissolved and particulate organic carbon (DOC, POC, POC% i.e. POC/suspended particulate matter:SPM), and phaeopigments (Phaeo). Samples were immediately filtered on-site through 0.2 μm filters. Filtrates were placed into acid-washed bottles (previously rinsed with filtrate aliquots), acidified when necessary, and stored at 4 °C in the dark pending analysis. Details on analytical procedures and techniques used for sample collection, handling and

analysis used are reported in SI, section S1.6. Analytical quality of the different methods applied for measurement of the metal dissolved concentrations was checked by analysis of Certified Reference Materials (CRMs; SI, section S1.6 and Table S4).

3. Results and discussion

3.1. Bio-physicochemical master variables and their temporal trends

The diel variations of the bio-physicochemical master variables, i.e. salinity, temperature: T, pH, dissolved oxygen saturation: O$_2$%, turbidity and chlorophyll *a* (chl*a*), were recorded *in situ* with the OS316 multiparameter probe. Furthermore, DOC, POC% and Phaeo were determined in the laboratory in collected samples. All data are reported in Fig. 2A–F. Temporal variation in salinity (Fig. 2A), ranging from 28.5 to 33.5, reflected typical semi-diurnal tide conditions of the site. Well-defined semi-diurnal cycles were also observed for T, pH, and DOC, reflecting a clear tide-dependence of these parameters. The variation in T (18.2–21.9 °C) and DOC (1.2–2 mg/L) were counter-cyclical to the diel variation in salinity (Fig. 2A, E). The maximum DOC concentrations occurred at low tide, suggesting allochthonous terrestrial DOC input (e. g. fulvic and humic acids) by the River Leyre and other freshwater effluents. The pH ranged from 7.8*5* and 8.0*3* with a semi-diurnal variation in phase with that of salinity (Fig. 2C). The temporal variation in dissolved oxygen saturation (88–105%; Fig. 2C) reflected tidal variations but also plankton photosynthetic/respiration activity as shown by the day/night contrast at low-tide. Maximum O$_2$ values match the maximum global insulation, while minimum O$_2$ coincides with maximum chl*a* during the night, see Fig. 2C and D. The turbidity data, expressed in nephelometric turbidity units (NTU), showed a tide-dependent trend with minimum value (2.3–2.7 NTU) at high tide and a higher value (9.5–10.5 NTU) at low tide (Fig. 2B). Interestingly, turbidity peaked at the beginning of flow-tide and at the end of the ebb-tide (2–3 h before and after low-tide; Fig. 2B). This suggests tidal sediment or fluid-mud resuspension, in line with low freshwater discharge and spring tide conditions that prevailed during the field monitoring, i.e. ideal conditions for sediment erosion and resuspension due to intensified variations in the boundary shear stress (Aguilar-Islas and Bruland, 2006; Jay and Dungan Smith, 1990).

Chl*a*, Phaeo, and POC% were analyzed for assessing phytoplankton biomass activities, status and influence on dynamic metal species (Abril et al., 2002; Axler and Owen, 1994). Chl*a* ranged from 0.3 to 3 μg/L reflecting significant phytoplankton biomass and activities (Fig. 2D). Maximum values for Chl*a* and Phaeo, non-photosynthetic pigments representative of algal chlorophyll pigments degradation, were observed at low tide. This and the moderate positive correlation between DOC and Chl*a* (r = 0.57; P < 0.01) as well as DOC and Phaeo (r = 0.53, P < 0.01) suggests the presence of biogenic material from freshwater allochthonous living and degraded phytoplankton cells, e.g. organic exudates, algae degradation material (Lancelot and Muylaert, 2011). The POC% ranging from 2 to 7.15% (Fig. 2F), also implies significant algal contribution to total POC% (Abril et al., 2002). The highest POC% coincided with highest Chl*a*, Phaeo, and turbidity values, suggesting a possible benthic algal-POC contribution after sediment resuspension (visualized by the turbidity peaks mentioned above).

3.2. Dynamic and total dissolved metal concentrations and their temporal variation

Observed temporal variations of Me$_{dyn}$ and Me$_{diss,}$ with the exception of Zn, are shown in (Fig. 2G–K). The results of Zn were not considered as Zn(II)$_{dyn}$ was mostly below the detection limit and contamination problems were suspected for the Zn(II)$_{diss}$ results. The observed temporal variations of Me$_{dyn}$ and Me$_{diss}$ have revealed clear element-specific differences in the temporal trends as well as in the relative amplitude of the temporal variations:
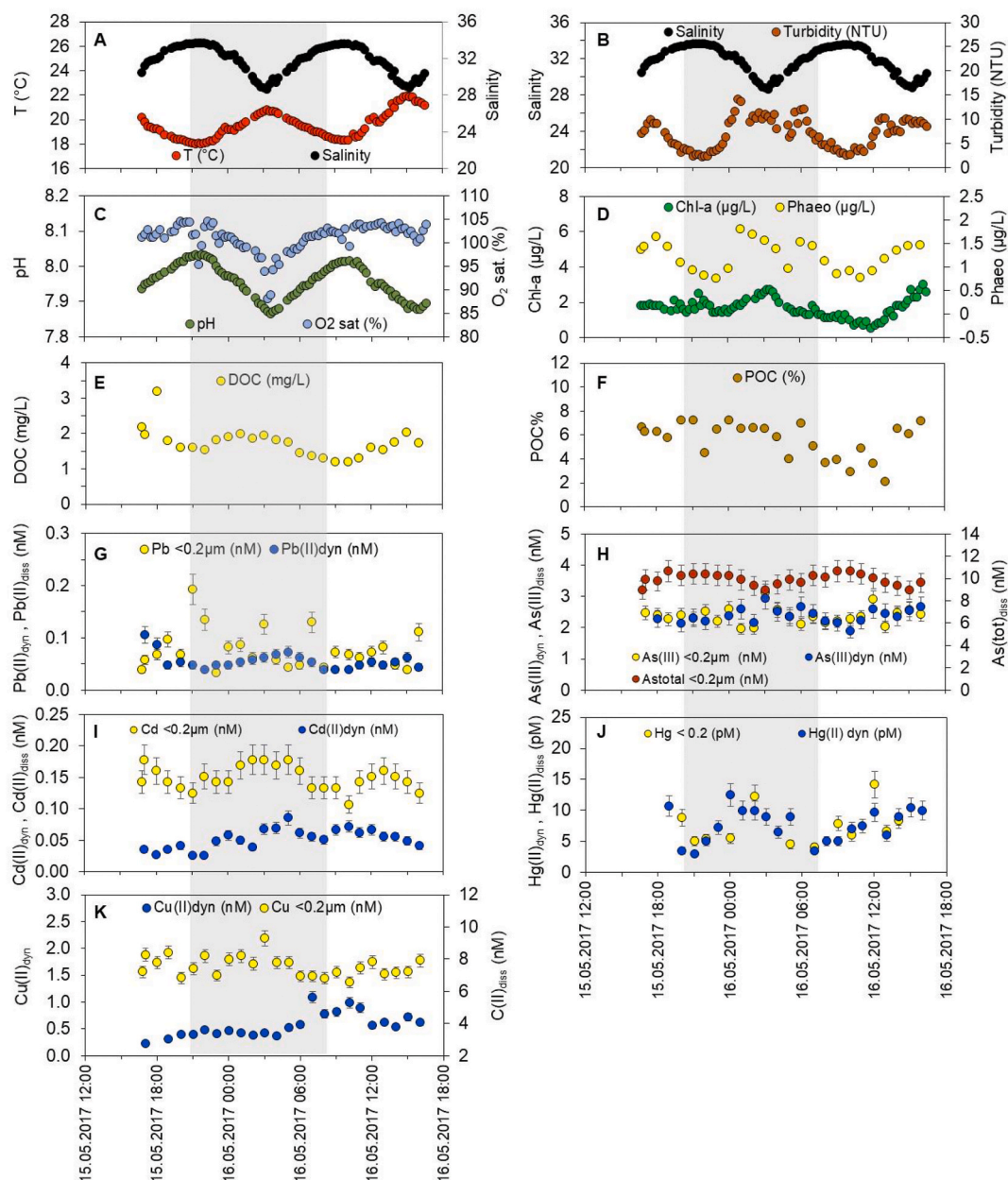
Fig. 2. Diel cycles of: A to D: master bio-physicochemical parameters; E–F: dissolved and particulate organic matters; G to K: Me$_{dyn}$ and Me$_{diss}$. Grey surface represents nighttime (solar radiation = 0). (See also ref (Tercier-Waeber et al., 2021). for data reported in B, E, J).

Lead. Pb(II)$_{dyn}$ ranged from 0.04 to 0.07 nM with significant hourly variations of up to 85% of Pb(II)$_{dyn}$ min (SI, Table S6), showing a trend counter-cyclical to salinity (Fig. 2A,G). Variations in Pb(II)$_{diss}$ (0.04–0.14 nM) were even more pronounced but without a clear temporal trend. Rather unlikely ratios Pb(II)$_{dyn}$ to Pb(II)$_{diss}$ > 120% (with considerable RSD values for the dissolved fraction) were obtained for samples collected at relatively high turbidity (>9 NTU), whereas Pb(II)$_{dyn}$ represented 40–80% of Pb(II)$_{diss}$ in samples collected at a turbidity < 7 NTU (SI, Table S6). This observation may suggest that for the most turbid samples, a significant proportion of Pb(II)$_{diss}$ might adsorb on the large amount of SPM retained at the membrane surface and is therefore lost during the sample filtration step. This hypothesis is supported by the known high affinity of Pb for inorganic particles and colloids (Dong et al., 2007; Tercier-Waeber et al., 2009).

Copper. The observed temporal variation in Cu(II)$_{dyn}$ ranged from 0.22 to 0.48 nM during the first tidal cycle and from 0.36 to 1.09 nM during the second one (Fig. 2K), suggesting a slightly increasing trend

throughout the measurement period. Cu(II)$_{diss}$ varied from 6.55 to 9.30 nM and was slightly lower at high tide (Fig. 2K). The Cu(II)$_{dyn}$ contribution to Cu(II)$_{diss}$ was equivalent to 4–15% (4–6% during the first tidal cycle; 5–15% during the second one; SI, Table S6), and the temporal variations observed during the 24 h measurement period represented up to 263% and 42% of the respective minimum values of Cu(II)$_{dyn}$ and Cu(II)$_{diss}$ (SI, Table S6).

Cadmium. Cd(II)$_{dyn}$ (0.026–0.085 nM) showed significant temporal variations (227% of minimum Cd(II)$_{dyn}$; SI, Table S6) with increasing values from the late afternoon on May 15th until May 16th early morning, and decreasing values onwards 10 a.m. on May 16th (Fig. 2I). Cd(II)$_{diss}$ ranged from 0.11 to 0.17 nM and revealed a temporal trend highly different than Cd(II)$_{dyn}$ (Fig. 2I). Minimum Cd(II)$_{diss}$ occurred at high tide and its maximum near low tide. Cd(II)$_{dyn}$ represented 22–57% of total Cd(II)$_{diss}$ and, as for Cu, the amplitude of temporal variations was very different, i.e. up to 227% for Cd(II)$_{dyn}$; up to 42% for Cd(II)$_{diss}$ (SI, Table S6).

Arsenite and arsenic. The presence of As(III) in oxic natural waters is thought to stem from As(V) phytoplankton uptake, due to the chemical similarity of As(V) with o-phosphate, and subsequent biotransformation and excretion of As(III) (Cervantes et al., 1994; Rahman et al., 2014). As(III)$_{dyn}$ and As(III)$_{diss}$ temporal concentration ranges (1.9–3.1 nM and 2–3.0 nM respectively; Fig. 2H) and trends (variation up to 57% and 50%; As(III)$_{dyn}$/As(III)$_{diss}$ ratios of 90–110%) were similar (see SI, Table S6). These results suggest that As(III) in the Arcachon Bay is mainly present in the dynamic form, and therefore potentially available for biota. Similar findings were made recently in the Gironde Estuary and the Elbe Estuary (Penezić et al., 2020; Tercier-Waeber et al., 2020). As(III)$_{dyn}$ (and As(III)$_{diss}$) temporal variation was tide-dependent, with a concentration minimum at high tide and a maximum around low tide. The temporal variation of As(tot)$_{diss}$, ranging from 8.9 to 10.7 nM, also reflected tidal dependence but with an opposite trend compared to As(III), i.e. maximum concentration occurred at high tide and minimum at low tide. These results suggest a source of As(III) mainly of terrestrial origin, while that of As(V) (i.e. As(tot)-As(III)) is mainly marine. As(III)$_{dyn}$ contributed 17–30% to As(tot)$_{diss}$ (SI, Table 6), i.e. roughly 3-fold more than in the Gironde Estuary during summer (5–10%; Penezić et al., 2020). This contribution is also higher than calculations predicting that 15–20% of dissolved As(V) can be reduced by phytoplankton during spring and summer blooms on the continental shelf (Cervantes et al., 1994; Rahman et al., 2014). This suggests that reduction of As(V) by phytoplankton in the water column might not be the only source of As(III). This is discussed in section 3.3.

Mercury. As observed for As(III) fractions, Hg(II)$_{dyn}$ and Hg(II)$_{diss}$ concentrations (3.4–12.5 pM and 4.1–14.1 pM respectively; Fig. 2J) and variation trends (Hg(II)$_{dyn}$/Hg(II)$_{diss}$ ratios 98 ± 25%; SI, Table S6) were similar when accounting for analytical errors. The recorded concentration levels were comparable to Hg(II)$_{diss}$ concentration ranges monitored with laboratory techniques in May 2006 (Bouchet et al., 2013). The temporal trend of the Hg(II) fractions were counter-cyclical to salinity (Fig. 2J). This suggests terrestrial sources of Hg(II) mainly in dynamic forms that are potentially available for bio-uptake.

3.3. Sources and biotic/abiotic processes controlling the temporal variation of the metal bioavailable fractions

The temporal variation of the Me$_{diss}$ fractions (Fig. 2H–K) showed clearly tide-dependent cycles, reflecting conservative behavior, except for Pb (Fig. 2G), probably due to analytical artifacts during filtration (see section 3.1). In contrast, the temporal trends of Me$_{dyn}$ were different, and generally more complex, than those of the total dissolved fractions except for Hg (Fig. 2G–K). These findings suggest that other processes, in addition to fresh- and seawater mixing, influence the temporal proportions and concentrations of the dynamic fraction of the metals studied.

Pearson's correlation coefficients r between Me$_{dyn}$ and master physicochemical parameters, organic contents and productivity proxies (turbidity, O$_2$%, DOC, POC%, Chl$a$, and Phaeo) were evaluated (Table 1) in order to assess abiotic and/or biotic processes controlling Me$_{dyn}$

temporal variations and identify Me$_{dyn}$ sources at monitored site. The parameters T and pH, reflecting mainly the mixing of the terrestrial and marine water bodies, were not considered. As dilution by mixing also influences the other parameters to some extent, the significant level (P-value) was fixed at 0.01, instead of the conventional 0.05, to interpret the correlation in terms of causation.

Lead. No significant correlation was observed between Pb(II)$_{dyn}$ and the master parameters considered. These results, coupled to the counter-cyclical trend with respect to salinity, suggest mainly fluvial origin of Pb(II)$_{dyn}$ at the monitored site and a conservative behaviour in the monitored salinity range, because the temporal variations of Pb(II)$_{dyn}$ are mainly due to the mixing of the two water bodies.

Copper. Cu(II)$_{dyn}$ was negatively correlated to DOC, but also to POC% and Chl$a$. This confirms the strong influence of organic materials on Cu binding and bioavailability as revealed by laboratory experiments and international speciation studies in fresh and marine (estuaries, coastal area) aquatic ecosystems (Dong et al., 2007; Illuminati et al., 2019; Louis et al., 2009; Tercier-Waeber et al, 2009, 2012). Since phytoplankton biomass contributed to the DOC and POC% pool (see section 3.1), it is plausible to assume a role of biogenic organic ligands in Cu binding (i.e. sorption on cell walls, Cu-binding exudates) and therefore on Cu(II)$_{dyn}$ temporal variation in the studied area. Cu adsorption on cell walls would explain the low Cu(II)$_{dyn}$ concentrations coinciding with the highest POC% values during the first tidal cycle (5pm to 4am; May 15–16), and the increase in Cu(II)$_{dyn}$ coinciding with POC%, Chl$a$ and DOC decrease (4am–~11am, May 16th). A 2-fold decrease in Cu(II)$_{dyn}$ and increase in Cu(II)$_{diss}$, coinciding with an increase in phytoplankton biomass (POC%) and production (Chl$a$), were observed on May 16th (10am–17pm; Fig. 2D, F, K). Phytoplankton exudation of Cu-binding extracellular polymeric substances (EPS) could explain these observations. In fact, as previously observed in freshwater streams (Tercier-Waeber et al., 2009), the free ligand sites on released EPS may outcompete the weak ligands of the dynamic Cu complexes, and thus decrease the proportion of this latter species.

Cadmium. Cd(II)$_{dyn}$ increased from early night to early morning and decreased during the day (Fig. 2I), being negatively correlated to O$_2$, a proxy for photosynthesis/respiration activities of living organisms, and to POC% standing for the presence of biomass (Table 1). These observations suggest reversible Cd sorption processes on living organisms due to pH changes at their surface induced by photosynthesis/respiration as reported in previous laboratory and field studies (Beck et al., 2009; Buffle and Tercier-Waeber, 2005; Tercier-Waeber et al., 2009). Namely, microsensor profiles of pH measured immediately above the benthic biofilm (0–1 mm) in a freshwater stream revealed that pH at the surface of active biomass may be up to 0.5 units lower during respiration (CO$_2$ release) and up to 1.5 units higher during photosynthesis (CO$_2$ uptake) compared to the pH ~8 of the water column (Beck et al., 2009), giving a total range of pH of 7.5–9.5. In Fig. 2C, respiration is associated to the O$_2$ decrease from midnight to 6am May 16th while photosynthesis increases O$_2$ from noon to 4pm on May 16th. Sorption studies on natural sorbent phases showed that change in pH of 7.5–9 may significantly influence Cd(II)$_{dyn}$ (and evidently Cd speciation) (Beck et al., 2009;

Table 1

Pearson's correlation coefficients (r) between the temporal variation of the dynamic metal fraction concentrations and selected bio-physicochemical master variables or dissolved and particulate organic matter and Chl$a$ concentrations at the Comprian site. Statistical significance level was set at 0.01 (p < 0.01).

	Pb(II)$_{dyn}$	Cd(II)$_{dyn}$	Cu(II)$_{dyn}$	As(III)$_{dyn}$	Hg(II)$_{dyn}$
Salinity	−0.40; P < 0.01	−0.18; P > 0.01	0.37; P < 0.01	−0.58; P < 0.01	−0.56; P < 0.01
Turbidity	0.22; P > 0.01	0.18; P > 0.01	−0.11; P > 0.01	0.64; P < 0.01	0.67; P < 0.01
O$_2$%	−0.03; P > 0.01	−0.60; P < 0.01	−0.18; P > 0.01	−0.23; P > 0.01	−0.02; P > 0.01
DOC	0.46; P > 0.01	−0.33; P > 0.01	−0.80; P < 0.01	0.08; P > 0.01	0.65; P < 0.01
POC%	0.28; P > 0.01	−0.54; P < 0.01	−0.56; P < 0.01	0.04; P > 0.01	0.24; P > 0.01
Chl$a$	0.04; P > 0.01	−0.19; P > 0.01	−0.54; P < 0.01	0.67; P < 0.01	0.12; P > 0.01

Interpretation correlation coefficient: $0.6 \leq |r| \leq 0.8$ - strong; $0.4 \leq |r| < 0.6$ - moderate; $0.2 \leq |r| < 0.4$ - weak; $0.0 \leq |r| < 0.2$ - very weak (www.slideshare.net/phannithr upp/guideline-for-interpreting-correlation-coefficient).

Tercier-Waeber et al., 2009). In contrast, a pH of <6.5 and < 5 would be needed to affect Pb and Cu adsorption, respectively (Buffle and Tercier-Waeber, 2005). The parallel variations in $Cd(II)_{dyn}$ and $Cd(II)_{diss}$ during respiration ($\Delta Cd_{dyn} = +0.035$ nM and $\Delta Cd(II)_{diss} = +0.036$ nM from midnight to 6am May 16th) and photosynthesis ($\Delta Cd(II)_{dyn} = -0.030$ nM and $\Delta Cd(II)_{diss} = -0.033$ nM from noon to 4 p.m. May 16th) further support reversible Cd sorption on phytoplankton induced by photosynthesis and respiration.

Arsenite. $As(III)_{dyn}$ was positively correlated to Chl*a*, supporting As$(III)_{dyn}$ excretion by phytoplankton in oxic waters, and to turbidity, consistent with the upstream freshwater effluents as a source of active phytoplankton (Fig. 2D). Significant increases of $As(III)_{dyn}$ coincided with turbidity peaks at the beginning of flow-tide and at the end of the ebb-tide, especially during the second semi-diurnal cycle. The turbidity peak was attributed to tidal mudflats resuspension (see section 3.1), which suggests a benthic As(III) remobilization. This is consistent with the ability of some sediment-dwelling bacteria to reduce As(V) to As(III) (Oremland et al., 2000; Plewniak et al., 2013), which is less particle reactive and, thus, more mobile than As(V) (Ahmann et al., 1997; Masson et al., 2007). Benthic contribution is also consistent with the observed $As(III)_{dyn}$ contribution of up to 34% relative to $As(tot)_{diss}$. Note that benthic remobilization might also influence the Cd_{dyn} temporal trends (Fig. 2I).

Mercury. $Hg(II)_{dyn}$ was positively correlated with DOC mainly derived from the upstream effluents (Fig. 2E), consistent with numerous studies showing that Hg and dissolved organic matter (DOM) are linked mechanistically and thus co-vary in aquatic systems (Lavoie et al., 2013). Moreover, DOM acts as a vector of Hg in the land-ocean aquatic continuum (Cesário et al., 2018). The similar observed $Hg(II)_{dyn}$ and Hg $(II)_{diss}$ concentrations (Fig. 2J) suggest that the Hg-DOM complexes present at the Comprian site are mainly in the dynamic form; i.e. sufficiently labile and mobile to be detected by AuNF-GIME interrogated by SWASV and therefore potentially bioavailable. The mobility of the Hg-DOM complexes is consistent with recent studies demonstrating that DOM in coastal water is dominated ($\geq 75\%$) by low molecular weight ($MW \leq 2$ kDa) hydrophilic fulvic-like organic matter (Shimotori et al., 2016). The size of these predominant DOM, based on their MW, can be estimated to be a few nanometers. Therefore, Hg(II) complexes with these DOM may diffuse through the gel and contribute to the observed dynamic Hg(II) fraction as very recently demonstrated by Tercier-Waeber et al. (2021). The lability of the Hg-DOM complexes is consistent with Hg(II) binding to the DOM weak functional groups (Chiasson-Gould et al., 2014; Miller et al., 2009). These weak functional groups are present in much larger concentrations than the strong sulfhydryl binding sites.

A positive correlation was also observed between $Hg(II)_{dyn}$ and turbidity, with a correlation coefficient r similar that between $Hg(II)_{dyn}$ and DOC (Table 1). This is consistent with a concomitant supply of Hg (II) and DOM by the freshwater upstream effluents of natural and anthropogenic origin (Fig. 2B,E,J). Moreover, as observed for $As(III)_{dyn}$, $Hg(II)_{dyn}$ was found to peak together with turbidity at the beginning of flow-tide and at the end of the ebb-tide, suggesting that tide-induced fluid-mud resuspension might play an important role in the release of $Hg(II)_{dyn}$ into the water column, increasing Hg exposure of the Arcachon Bay ecosytem.

3.4. Implications for environmental monitoring and policy

The TracMetal enables to detect *in situ*, and therefore with minimal analytical artifacts, subtle variations of the potentially bioavailable fractions of a range of hazardous trace metals in dynamic aquatic ecosystems. The TracMetal may thus serve as a real-time sentinel system for tracing hazardous metal species sources and fate, and for ecotoxicological risk assessment. Temporal variation of the potentially bioavailable metal species can be decoupled from those of the total dissolved metal species as measured in filtered samples. The proportion of the dynamic species depends on the metal and the surrounding bio-physicochemical conditions and may vary from a few % (e.g. Cu) to close to 100% (e.g As(III) and Hg(II)). While the total dissolved metal concentrations were mainly tide-dependent, different biotic and abiotic processes controlled the temporal variation of the dynamic Pb, Cu, Cd, As(III) and Hg(II) fractions in the Arcachon Bay. The temporal cycling of $As(III)_{dyn}$, $Cu(II)_{dyn}$ and $Cd(II)_{dyn}$ appear to be controlled by biological cycles including, respectively, (i) phytoplankton excretion or lysis; (ii) complexation with excreted organic matter and/or (iii) reversible adsorption by algal cells, whereas $Pb(II)_{dyn}$ and $Hg(II)_{dyn}$ showed conservative behavior. Tidal mudflats contributed measurable $Hg(II)_{dyn}$ and $As(III)_{dyn}$ (and possibly $Cd(II)_{dyn}$) of benthic origin to the water column.

The metal concentrations monitored was compared with Acute Water Quality Criteria (WQC) trigger values derived in an attempt to protect a pre-determined percentage of living species (ANZECC, 2000). $Cu(II)_{diss}$ (ranging from 9.3 to 6.5 nM) and $As(V)_{diss}$ (determined by subtraction of $As(III)_{diss}$ to $As(tot)_{diss}$ and ranging from 6.6 to 9.6 nM) were respectively highest and similar to the WQC to protect 99% of the biota (i.e. 4.7 nM and 10 nM for Cu(II) and As(V), respectively). This reflects that these two metals have a potential for causing adverse impacts that should be verified and tailored to local communities, taking into account not only their total concentrations but also the concentration of their dynamic fraction. This also indicates that addition of these two metals in the revised EU Priority Substances Daughter Directive should be evaluated.

International environmental administration bodies recently stated the need to quantify the potentially bioavailable fraction of hazardous trace metals instead of just their total dissolved concentrations. This will support the establishment of environmental quality standards (EQS) and guidelines (EQG) based on realistic risk assessment to protect aquatic life and resources, and ultimately human health. The original findings of this work support the need of this paradigm shift.

CRediT author statement

Declaration of competing interest

The authors declare that they have no known competing financial interests or personal relationships that could have appeared to influence the work reported in this paper.

Acknowledgements

Appendix A. Supplementary data

Supplementary data to this article can be found online at https://doi.

org/10.1016/j.chemosphere.2021.131014.

References

Abril, G., Nogueira, M., Etcheber, H., Cabeçadas, G., Lemaire, E., Brogueira, M.J., 2002. Behaviour of organic carbon in nine contrasting European estuaries. Estuarine. Coast. Shelf Sci. 54, 241–262. https://doi.org/10.1006/ecss.2001.0844.

Aguilar-Islas, A.M., Bruland, K.W., 2006. Dissolved manganese and silicic acid in the Columbia River plume: a major source to the California current and coastal waters off Washington and Oregon. Mar. Chem. 101, 233–247. https://doi.org/10.1016/j.marchem.2006.03.005.

Ahmann, D., Krumholz, L.R., Hemond, H.F., Lovley, D.R., Morel, F.M.M., 1997. Microbial mobilization of arsenic from sediments of the aberjona watershed. Environ. Sci. Technol. 31, 2923–2930. https://doi.org/10.1021/es970124k.

Ainla, A., Mousavi, M.P.S., Tsaloglou, M.-N., Redston, J., Bell, J.G., Fernández-Abedul, M.T., Whitesides, G.M., 2018. Open-source potentiostat for wireless electrochemical detection with smartphones. Anal. Chem. 90, 6240–6246. https://doi.org/10.1021/acs.analchem.8b00850.

Anderson, R., Mawji, E., Cutter, G., Measures, C., Jeandel, C., 2014. GEOTRACES: changing the way we explore ocean chemistry. oceanog, 27, pp. 50–61.

ANZECC, 2000. ANZECC, Australian and New Zealand Guidelines for Fresh and Marine Water Quality. Australian and New Zealand Environment and Conservation Council, Canberra (2000). http://www.mincos.gov.au/publication/national_water_quality_management_strategy.

Axler, R.P., Owen, C.J., 1994. Measuring chlorophyll and phaeophytin : whom should you believe ? Lake Reservoir Manag. 8, 143–151.

Baeyens, W., Bowie, A.R., Buesseler, K., Elskens, M., Gao, Y., Lamborg, C., Leermakers, M., Remenyi, T., Zhang, H., 2011. Size-fractionated labile trace elements in the northwest pacific and southern oceans. Mar. Chem. 126, 108–113. https://doi.org/10.1016/j.marchem.2011.04.004.

Baeyens, W., Gao, Y., Davison, W., Galceran, J., Leermakers, M., Puy, J., Superville, P.-J., Beguery, L., 2018. In situ measurements of micronutrient dynamics in open seawater show that complex dissociation rates may limit diatom growth. Sci. Rep. 8, 16125. https://doi.org/10.1038/s41598-018-34465-w.

Beck, A.J., Janssen, F., Polerecky, L., Herlory, O., de Beer, D., 2009. Phototrophic biofilm activity and dynamics of diurnal Cd cycling in a freshwater stream. Environ. Sci. Technol. 43, 7245–7251. https://doi.org/10.1021/es900069y.

Belmont-Hébert, C., Tercier, M.L., Buffle, J., Fiaccabrino, G.C., de Rooij, N.F., Koudelka-Hep, M., 1998. Gel-integrated microelectrode arrays for direct voltammetric measurements of Heavy metals in natural waters and other complex Media. Anal. Chem. 70, 2949–2956. https://doi.org/10.1021/ac971194c.

Bouchet, S., Amouroux, D., Rodriguez-Gonzalez, P., Tessier, E., Monperrus, M., Thouzeau, G., Clavier, J., Amice, E., Deborde, J., Bujan, S., Grall, J., Anschutz, P., 2013. MMHg production and export from intertidal sediments to the water column of a tidal lagoon (Arcachon Bay, France). Biogeochemistry 114, 341–358. https://doi.org/10.1007/s10533-012-9815-z.

Braungardt, C.B., Achterberg, E.P., Axelsson, B., Buffle, J., Graziottin, F., Howell, K.A., Illuminati, S., Scarponi, G., Tappin, A.D., Tercier-Waeber, M.-L., Turner, D., 2009. Analysis of dissolved metal fractions in coastal waters: an inter-comparison of five voltammetric in situ profiling (VIP) systems. Mar. Chem. 114, 47–55. https://doi.org/10.1016/j.marchem.2009.03.006.

Bruland, K.W., Middag, R., Lohan, L.C., 2013. Controls of Trace Metals in Seawater, in: Treatise on Geochemistry, second ed. Saunders, Elsevier Inc., Philadelphia, USA, pp. 19–51.

Buffle, J., Tercier-Waeber, M.-L., 2005. Voltammetric environmental trace-metal analysis and speciation: from laboratory to in situ measurements. TrAC Trends in analytical chemistry. Trace-Metal Anal. 24, 172–191. https://doi.org/10.1016/j.trac.2004.11.013.

Buffle, J., Tercier-Waeber, M.-L., 2000. In situ voltammetry: concepts and practice for trace analysis and speciation, chap. 9. In: In Situ Monitoring of Aquatic Systems; Chemical Analysis and Speciation, IUPAC Series. Wiley, Chichester.

Buffle, J., Wilkinson, K.J., van Leeuwen, H.P., 2009. Chemodynamics and bioavailability in natural waters. Environ. Sci. Technol. 43, 7170–7174. https://doi.org/10.1021/es9013695.

Cervantes, C., Ji, G., Ramírez, J.L., Silver, S., 1994. Resistance to arsenic compounds in microorganisms. FEMS Microbiol. Rev. 15, 355–367. https://doi.org/10.1111/j.1574-6976.1994.tb00145.x.

Cesário, R., Mota, A.M., Caetano, M., Nogueira, M., Canário, J., 2018. Mercury and methylmercury transport and fate in the water column of Tagus estuary (Portugal). Mar. Pollut. Bull. 127, 235–250. https://doi.org/10.1016/j.marpolbul.2017.11.066.

Chiasson-Gould, S.A., Blais, J.M., Poulain, A.J., 2014. Dissolved organic matter kinetically controls mercury bioavailability to bacteria. Environ. Sci. Technol. 48, 3153–3161. https://doi.org/10.1021/es4038484.

Dong, D., Liu, L., Hua, X., Lu, Y., 2007. Comparison of lead, cadmium, copper and cobalt adsorption onto metal oxides and organic materials in natural surface coatings. Microchem. J. 85, 270–275. https://doi.org/10.1016/j.microc.2006.06.015.

Durán, I., Beiras, R., 2013. Ecotoxicologically based marine acute water quality criteria for metals intended for protection of coastal areas. Sci. Total Environ. 463–464, 446–453. https://doi.org/10.1016/j.scitotenv.2013.05.077.

Fighera, M., Wal, P.D.V. der, Tercier-Waeber, M.-L., Shea, H., 2016. Three-electrode on-chip sensors for voltammetric detection of trace metals in natural waters. ECS Trans. 75, 303. https://doi.org/10.1149/07516.0303ecst.

Gaillardet, J., Viers, J., Dupré, B., 2003. Trace Elements in River Waters, in: Treatise on Geochemistry. Elsevier, pp. 225–272. https://doi.org/10.1016/B0-08-043751-6/05165-3.

Grand, M.M., Laes-Huon, A., Fietz, S., Resing, J.A., Obata, H., Luther, G.W., Tagliabue, A., Achterberg, E.P., Middag, R., Tovar-Sánchez, A., Bowie, A.R., 2019. Developing autonomous observing systems for micronutrient trace metals. Front. Mar. Sci. 6, 35. https://doi.org/10.3389/fmars.2019.00035.

Illuminati, S., Annibaldi, A., Truzzi, C., Tercier-Waeber, M.-L., Nöel, S., Braungardt, C.B., Achterberg, E.P., Howell, K.A., Turner, D., Marini, M., Romagnoli, T., Totti, C., Confalonieri, F., Graziottin, F., Buffle, J., Scarponi, G., 2019. In-situ trace metal (Cd, Pb, Cu) speciation along the Po River plume (Northern Adriatic Sea) using submersible systems. Mar. Chem. 212, 47–63. https://doi.org/10.1016/j.marchem.2019.04.001.

Jay, D.A., Dungan Smith, J., 1990. Circulation, density distribution and neap-spring transitions in the Columbia River Estuary. Prog. Oceanogr. 25, 81–112. https://doi.org/10.1016/0079-6611(90)90004-L.

Lancelot, C., Muylaert, K., 2011. 7.02 - trends in estuarine phytoplankton ecology. In: Wolanski, E., McLusky, D. (Eds.), Treatise on Estuarine and Coastal Science. Academic Press, Waltham, pp. 5–15. https://doi.org/10.1016/B978-0-12-374711-2.00703-8.

Lavoie, R.A., Jardine, T.D., Chumchal, M.M., Kidd, K.A., Campbell, L.M., 2013. Biomagnification of mercury in aquatic food webs: a worldwide meta-analysis. Environ. Sci. Technol. 47, 13385–13394. https://doi.org/10.1021/es403103t.

Louis, Y., Garnier, C., Lenoble, V., Mounier, S., Cukrov, N., Omanović, D., Pižeta, I., 2009. Kinetic and equilibrium studies of copper-dissolved organic matter complexation in water column of the stratified Krka River estuary (Croatia). Mar. Chem. 114, 110–119. https://doi.org/10.1016/j.marchem.2009.04.006.

Luoma, S.N., Rainbow, P.S., 2011. Metal Contamination in Aquatic Environments: Science and Lateral Management, paperback ed., vol. 1. Cambridge Univ. Press, Cambridge.

Maldonato, M.T., Hughes, M.P., Rue Eden, L., 2002. The effect of Fe and Cu on growth and domoic acid production by Pseudo-nitzschia multiseries and Pseudo-nitzschia australis. Limnol. Oceanogr. 47, 515–526.

Masson, M., Schäfer, J., Blanc, G., Pierre, A., 2007. Seasonal variations and annual fluxes of arsenic in the garonne, dordogne and isle rivers, France. Sci. Total Environ. 373, 196–207. https://doi.org/10.1016/j.scitotenv.2006.10.039.

Merrington, G., Peters, A., Schlekat, C.E., 2016. Accounting for metal bioavailability in assessing water quality: a step change?: metal bioavailability and water quality. Environ. Toxicol. Chem. 35, 257–265. https://doi.org/10.1002/etc.3252.

Miller, C.L., Southworth, G., Brooks, S., Liang, L., Gu, B., 2009. Kinetic controls on the complexation between mercury and dissolved organic matter in a contaminated environment. Environ. Sci. Technol. 43, 8548–8553. https://doi.org/10.1021/es901891t.

Morel, F.M.M., Milligan, A.J., Saito, M.A., 2003. Marine bioinorganic chemistry: the role of trace metals in the oceanic cycles of major nutrients. In: The Oceans and Marine Geochemistry. Elsevier, Oxford, pp. 113–143.

Oremland, R.S., Dowdle, P.R., Hoeft, J.O., Sharp, J.O., Schaefer, J.K., Miller, L.G., Switzer Blum, J., Smith, R.L., Bloom, N.S., Wallschlaeger, D., 2000. Bacterial dissimilatory reduction of arsenate and sulfate in meromictic Mono Lake. Geochem. Cosmochim. Acta 64, 3073–3084.

Penezić, A., Tercier-Waeber, M.-L., Abdou, M., Bossy, C., Dutruch, L., Bakker, E., Schäfer, J., 2020. Spatial variability of arsenic speciation in the Gironde Estuary: emphasis on dynamic (potentially bioavailable) inorganic arsenite and arsenate fractions. Mar. Chem. 223, 103804. https://doi.org/10.1016/j.marchem.2020.103804.

Plewniak, F., Koechler, S., Navet, B., Dugat-Bony, É., Bouchez, O., Peyret, P., Séby, F., Battaglia-Brunet, F., Bertin, P.N., 2013. Metagenomic insights into microbial metabolism affecting arsenic dispersion in Mediterranean marine sediments. Mol. Ecol. 22, 4870–4883. https://doi.org/10.1111/mec.12432.

Rahman, M.A., Hogan, B., Duncan, E., Doyle, C., Krassoi, R., Rahman, M.M., Naidu, R., Lim, R.P., Maher, W., Hassler, C., 2014. Toxicity of arsenic species to three freshwater organisms and biotransformation of inorganic arsenic by freshwater phytoplankton (Chlorella sp. CE-35). Ecotoxicol. Environ. Saf. 106, 126–135. https://doi.org/10.1016/j.ecoenv.2014.03.004.

Shimotori, K., Satou, T., Imai, A., Kawasaki, N., Komatsu, K., Kohzu, A., Tomioka, N., Shinohara, R., Miura, S., 2016. Quantification and characterization of coastal dissolved organic matter by high-performance size exclusion chromatography with ultraviolet absorption, fluorescence, and total organic carbon analyses: size and characterization of coastal DOM. Limnol Oceanogr. Methods 14, 637–648. https://doi.org/10.1002/lom3.10118.

Sigg, L., Black, F., Buffle, J., Cao, J., Cleven, R., Davison, W., Galceran, J., Gunkel, P., Kalis, E., Kistler, D., Martin, M., Noël, S., Nur, Y., Odzak, N., Puy, J., van Riemsdijk, W., Temminghoff, E., Tercier-Waeber, M.-L., Toepperwien, S., Town, R.M., Unsworth, E., Warnken, K.W., Weng, L., Xue, H., Zhang, H., 2006. Comparison of analytical techniques for dynamic trace metal speciation in natural freshwaters. Environ. Sci. Technol. 40, 1934–1941. https://doi.org/10.1021/es051245k.

Sunda, W.G., 2012. Feedback interactions between trace metal nutrients and phytoplankton in the ocean. Front. Microbiol. 3 https://doi.org/10.3389/fmicb.2012.00204.

Tercier, M.-L., Buffle, J., 1996. Antifouling membrane-covered voltammetric microsensor for in situ measurements in natural waters. Anal. Chem. 68, 3670–3678. https://doi.org/10.1021/ac960265p.

Tercier, M.-L., Buffle, J., Graziottin, F., 1998. A novel voltammetric in situ profiling system for continuous, real-time monitoring of trace elements in natural waters. Electroanalysis 10, 355–363. https://doi.org/10.1002/(SICI)1521-4109(199805)10:6<355::AIDELAN355>.3.0.CO;2-F.

Tercier-Waeber, M.-L., Abdou, M., Fighera, M., Kowal, J., Bakker, E., van der Wal, P., 2021. In situ voltammetric sensor of potentially bioavailable inorganic mercury in

marine aquatic systems based on gel-integrated nanostructured gold-based microelectrode arrays. ACS Sens. submit.

Tercier-Waeber, M.-L., Buffle, J., 2000. Submersible online oxygen removal system coupled to an in situ voltammetric probe for trace element monitoring in freshwater. Environ. Sci. Technol. 34, 4018–4024. https://doi.org/10.1021/es000033e.

Tercier-Waeber, M.-L., Buffle, J., Koudelka-Hep, M., Graziottin, F., 2002. Submersible voltammetric probes for in situ real-time trace element monitoring in natural aquatic systems. In: Environmental Electrochemistry:Analysis of Trace Element Biogeochemistry, ACS Symposium Series. American Chemical Society, Washington DC, USA.

Tercier-Waeber, M.-L., Confalonieri, F., Koudelka-Hep, M., Dessureault-Rompré, J., Graziottin, F., Buffle, J., 2008. Gel-integrated voltammetric microsensors and submersible probes as reliable tools for environmental trace metal analysis and speciation. Electroanalysis 20, 240–258. https://doi.org/10.1002/elan.200704067.

Tercier-Waeber, M.-L., Fighera, M., Abdou, M., Bakker, E., der Wal, P. van, 2020. Newly designed gel-integrated nanostructured gold-based interconnected microelectrode arrays for continuous in situ arsenite monitoring in aquatic systems. Sensor. Actuator. B Chem., 128996 https://doi.org/10.1016/j.snb.2020.128996.

Tercier-Waeber, M.-L., Hezard, T., Masson, M., Schäfer, J., 2009. In situ monitoring of the diurnal cycling of dynamic metal species in a stream under contrasting

photobenthic biofilm activity and hydrological conditions. Environ. Sci. Technol. 43, 7237–7244. https://doi.org/10.1021/es900247y.

Tercier-Waeber, M.-L., Stoll, S., Slaveykova, V.I., 2012. Trace metal behavior in surface waters: emphasis on dynamic speciation, sorption processes and bioavailability. Archive des Sci. 65, 119–142.

Tercier-Waeber, M.-L., Taillefert, M., 2008. Remote in situ voltammetric techniques to characterize the biogeochemical cycling of trace metals in aquatic systems. J. Environ. Monit. 10, 30–54. https://doi.org/10.1039/B714439N.

Touilloux, R., Tercier-Waeber, M.-L., Bakker, E., 2015. Antifouling membrane integrated renewable gold microelectrode for in situ detection of As(III). Anal. Method. 7, 7503–7510. https://doi.org/10.1039/C5AY01941A.

Väänänen, K., Leppänen, M.T., Chen, X., Akkanen, J., 2018. Metal bioavailability in ecological risk assessment of freshwater ecosystems: from science to environmental management. Ecotoxicol. Environ. Saf. 147, 430–446. https://doi.org/10.1016/j.ecoenv.2017.08.064.

van Leeuwen, H.P., Town, R.M., Buffle, J., Cleven, R.F.M.J., Davison, W., Puy, J., van Riemsdijk, W.H., Sigg, L., 2005. Dynamic speciation analysis and bioavailability of metals in aquatic systems. Environ. Sci. Technol. 39, 8545–8556. https://doi.org/10.1021/es050404x.

Zhao, C.-M., Campbell, P.G.C., Wilkinson, K.J., 2016. When are metal complexes bioavailable? Environ. Chem. 13, 425. https://doi.org/10.1071/EN15205.